JOURNAL OF VIROLOGY, Nov. 2005, p. 14235–14243 Vol. 79, No. 22
0022-538X/05/$08.00+0 doi:10.1128/JVI.79.22.14235–14243.2005

Mutation of a Single Conserved Nucleotide between the Cloverleaf and Internal Ribosome Entry Site Attenuates Poliovirus Neurovirulence

Nidia De Jesus, David Franco, Aniko Paul, Eckard Wimmer, and Jeronimo Cello*

Department of Molecular Genetics and Microbiology, School of Medicine, Stony Brook University, Stony Brook, New York 11794-5222

Received 3 June 2005/Accepted 19 August 2005

The chemical synthesis of poliovirus (PV) cDNA combined with the cell-free synthesis of infectious particles yielded virus whose mouse neurovirulence was highly attenuated (J. Cello, A. V. Paul, and E. Wimmer, Science 297:1016–1018, 2002). Compared to the wild-type PV1 (Mahoney) [PV1(M)] sequence, the synthetic virus genome harbored 27 nucleotide (nt) changes deliberately introduced as genetic markers. Of the 27 nucleotide substitutions, the UA-to-GG exchanges at nucleotides 102/103, mapping to a region between the cloverleaf and the internal ribosome entry site (IRES) in the 5′-nontranslated region, were found to be involved in the observed attenuation phenotype in mice. The UA/GG mutation at nt 102/103 in the synthetic PV1(M) [sPV1(M)] background conferred also a ts phenotype of replication to the virus in human neuroblastoma cells. Conversely, the exchange of GG to wild-type (wt) UA at 102/103 in an sPV1(M) background restored wt neurovirulence in *CD155* transgenic (tg) mice and suppressed the ts phenotype in SK-N-MC cells. All poliovirus variants replicated well in HeLa cells at the two temperatures, regardless of the sequence at the 102/103 locus. Analyses of variants isolated from sPV(M)-infected *CD155* tg mice revealed that the $G_{102}G_{103}$-to-$G_{102}A_{103}$ reversion alone reestablished the neurovirulent phenotype. This suggests that a single mutation is responsible for the observed change of the neurovirulence phenotype. sPV1(M) RNA is translated in cell extracts of SK-N-MC cells with significantly lower efficiency than PV1(M) RNA or sPV1(M) RNA with a G_{102}-to-A_{102} reversion. These studies suggest a function for the conserved nucleotide (A_{103}) located between the cloverleaf and the IRES which is important for replication of PV in the central nervous system of *CD155* tg mice and in human cells of neuronal origin.

Although the chemical synthesis of poliovirus (PV) cDNA combined with the cell-free synthesis of infectious particles has received much attention (7), the phenotypic properties of the synthetic virus have been largely ignored. The published sequence guiding the synthesis of the synthetic virus was that of a highly neurovirulent wild-type (wt) strain, poliovirus type 1 (Mahoney) [wt PV1(M)] (24, 43). To distinguish the synthetic virus [sPV1(M)] from PV1(M), we engineered 27 nucleotide changes into the sPV1(M) genome as genetic markers (7). Compared to the wt progenitor PV1(M) strain, the sPV1 derivative was, surprisingly, highly attenuated in transgenic mice (7) expressing the poliovirus receptor, *CD155* tg mice, which have been constructed by Koike et al. (25). It was plausible that one or several of the nucleotide changes that had been introduced into the sPM1(M) genome altered the neurovirulence of sPV1(M).

PV is a neurovirulent member virus of the genus *Enterovirus* in the family *Picornaviridae*. It is not yet known where the virus replicates in the gastrointestinal (GI) tract after enteric infection, but secondary lymphatic tissues most likely play a major role (21, 30, 33). Invasion of PV into the central nervous system is rare and altogether not necessary for viral dissemination in the population (33). Indeed, the ratio of infection to neurological complications in PV infections is very low (10^{-2} to 10^{-3}, depending upon the virus type). Upon invasion of the central nervous system, PV targets predominantly motor neurons for destruction, which leads to paralysis and even death (33). Only humans and nonhuman primates can be infected with PV, although humans are the only natural hosts of the virus. This host range restriction is related to CD155, the only known PV receptor (33). Construction of *CD155* tg mice, however, has allowed studies of PV pathogenesis (25, 45) in these animals. We are using *CD155* tg mice originally constructed by A. Nomoto and his colleagues (PVRTg21) (25). The *CD155* tg mice can be infected by the intramuscular, intravenous, or intracerebral route, but they are resistant to oral infection. The reason for this restriction is that the *CD155* gene is not expressed under the control of the human promoter in the GI tract of these animals (21, 61). The unexplained silence of the human *CD155* promoter in the mouse GI tract prevents studies of the first crucial steps in PV enteric infection in the *CD155* transgenic animals.

The genome of PV, which is of plus-strand polarity, is ~7,441 nucleotides (nt) long. It carries a small protein, VPg, covalently attached to its 5′ end (10, 29) and is polyadenylated at its 3′ end (60).

The genome consists of a long 5′-nontranslated region (NTR), a single large open reading frame, and a short 3′NTR (24, 58). Functionally, the 5′NTR can be divided into two regions: the 5′-terminal cloverleaf (nt 1 to 89) and the internal ribosomal entry site (IRES; nt 123 to 602) (58). Polyprotein synthesis is initiated 164 nt downstream of the IRES element at nt 743 (9, 58). The cloverleaf is an essential *cis*-acting signal in viral RNA replication (3, 37), while the IRES element controls cap-independent translation of the viral mRNA (22, 23,

* Corresponding author. Mailing address: Department of Molecular Genetics and Microbiology, School of Medicine, Stony Brook University, Life Sciences Bldg., Stony Brook, NY 11794-5222. Phone: (631) 632-4432. Fax: (631) 632-8891. E-mail: jcello@ms.cc.sunysb.edu.

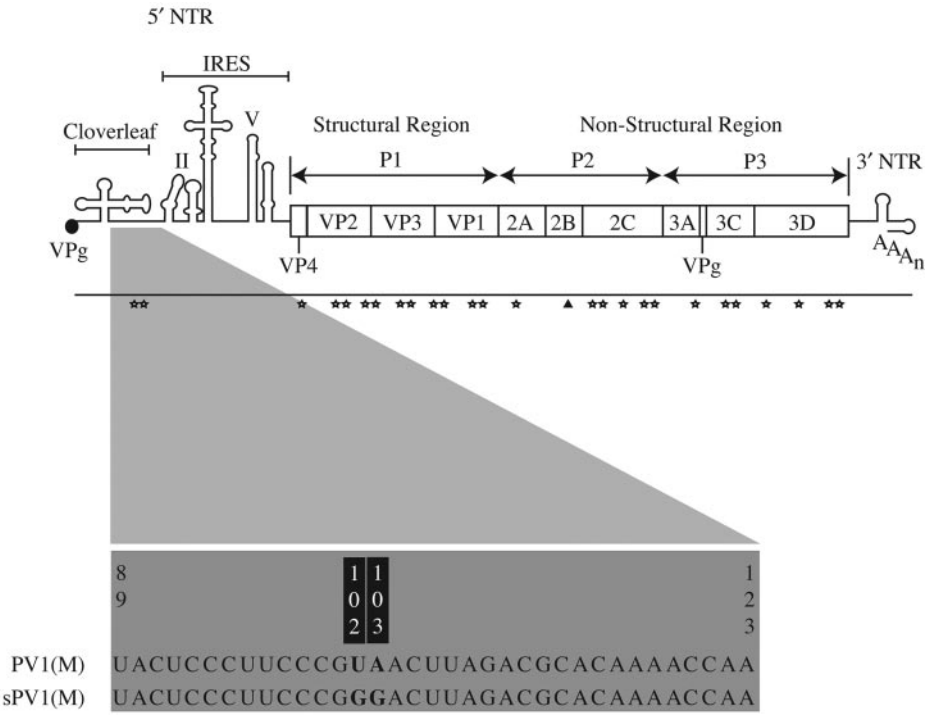

FIG. 1. Genomic structure of PV1(M). The 5′ end is terminated with the genome-linked protein VPg, and the 3′ end terminates with poly(A). The 5′NTR, harboring the cloverleaf and the IRES, is followed by the single open reading frame (open box) encoding the viral polyprotein and by the 3′NTR. The polyprotein contains (N terminus to C terminus) structural (P1) and nonstructural (P2 and P3) proteins that are released from the polypeptide chain by proteolytic processing (58). The stars beneath the genome indicate the presence of 27 nucleotide substitutions originally engineered into sPV1(M) as a means of differentiating sPV1(M) from PV1(M). The filled triangle represents the only substitution resulting in a nonsynonymous amino acid change in sPV1(M). The insert shows the nucleotide sequences of PV1(M) and sPV1(M) in the spacer region between the cloverleaf and the IRES (nt 89 to 123) and highlights in bold two nucleotide substitutions ($U_{102}G$ and $A_{103}G$) originally engineered into the sPV1(M) strain.

39, 40). The two highly structured control elements are separated by 35 nucleotides that, so far, have not been assigned to any function in viral proliferation. No binding partners of these nucleotides with upstream or downstream nucleotides have been suggested and, thus, it is currently being assumed that these 35 nucleotides present a single-stranded spacer between the cloverleaf and the IRES (Fig. 1).

The 27 nucleotide substitutions introduced into sPV1(M) mapped predominantly to the open reading frame of the polyprotein and, with the exception of one nonsynonymous change in the coding region for protein 2B, they were "silent mutations" (Fig. 1). The nonsynonymous mutation in 2B has been shown previously to exert no replication phenotype in HeLa cells (26). Two mutations ($U_{102}A_{103}$ to $G_{102}G_{103}$) mapped to the 5′NTR, specifically to the spacer region between the cloverleaf and the IRES (Fig. 1). Again, these mutations have been shown not to influence the replication of poliovirus in HeLa cells (31, 59). We assumed, perhaps naively, that none of the 27 nucleotide changes would affect replication and/or the pathogenic potential of sPV1. This assumption was wrong (7). Although sPV1(M) replicates with nearly wt kinetics in HeLa cell cultures, neurological symptoms (paralysis) after infection of *CD155* tg mice were observed only with a dose of sPV1(M) that was 10^4 in excess of the dose required for PV1(M) (7). In this study, we have analyzed the remarkable attenuation phenotype of sPV1(M). We have observed that sPV1(M) expressed a severe ts phenotype at 39.5°C in cells of human neuronal origin (SK-N-MC cells), a phenomenon not seen in HeLa cells. We describe here that both genetic traits, the attenuation phenotype in *CD155* tg mice as well as the ts phenotype in SK-N-MC cells, covary with the nucleotide substitutions at the 102/103 locus (UA to GG) of the 5′NTR. Analyses of revertants isolated from *CD155* tg mice infected with sPV1(M) further narrowed the locus responsible for both genetic traits to a single A-to-G transition at nt 103.

We will provide preliminary evidence suggesting that the phenotypic effect of these mutations in a region of the viral genome previously not assigned to any function is likely related to a defect in translation.

MATERIALS AND METHODS

Plasmid constructions. sPV1(M) originated from a full-length poliovirus type 1 cDNA which was chemically synthesized by assembling oligonucleotides of plus- and minus-strand polarities according to the sequence of PV1(M), as described previously (7). The genomic structure of PV1(M), as depicted in Fig. 1, indicates 27 nucleotide changes introduced into the cDNA as genetic markers. The sPV1(M) cDNA also carries a T7 RNA promoter at the 5′NTR end for synthesis of infectious RNA (57).

pT7PV1(M) is the progenitor plasmid containing the full-length cDNA of *PV1(M)* (57). Recombinants between PV1(M) and sPV1(M) were constructed to determine the contributions of mutations responsible for the attenuated phenotype of sPV1(M). pT7PV1(M), which contained the PV1(M) genome, and pBR322-sPV1(M), which contained the sPV1(M) genome, were digested with EcoRI and StuI, which restrict within the vectors and at position 3836 within the

PV1(M) and sPV1(M) genomes, respectively. Subsequent exchanges of resulting fragments resulted in the generation of viral variants sPV1(M)-PV1(M) and PV1(M)-sPV1(M). In sPV1(M)-PV1(M), the second half of the sPV1(M) genome was exchanged for that of PV1(M). In PV1(M)-sPV1(M), the second half of the PV1(M) genome was exchanged for that of sPV1(M).

UA sPV1(M) cDNA is a derivative of sPV1(M) cDNA carrying wild-type UA nucleotides at the 102/103 locus in the 5′NTR. UA sPV1(M) cDNA was constructed by replacing an EcoRI-AgeI fragment of sPV1(M) cDNA (vector to nt 339 of the PV sequence, including T7 promoter sequence) that is 405 nucleotides long, by the respective EcoRI-AgeI fragment of pT7PV1(M). GG PV1(M) cDNA, the wt cDNA carrying GG at the 102/103 locus, was constructed by replacing the EcoRI-AgeI fragment of pT7PV1(M) with the respective EcoRI-AgeI fragment of sPV1(M) cDNA.

GA PV1(M) cDNA carrying the G-to-A reversion at position 103 was generated by site-directed mutagenesis using GG PV1(M) cDNA as a template. A PCR fragment was synthesized with oligonucleotides PVPSA103 (5′-ATACTC CCTTCCCGGAACTTAGACGCACAAAACC-3′; plus-strand sequence) and 283 MS (5′-GGTTGAGTGCTGAGCGC-3′; minus-strand sequence). A second PCR fragment was synthesized with oligonucleotides PVMSA103 (5′-TTTGTG CGTCTAAGTTCCGGGAAGGGAGTATAAAAC-3′; minus-strand sequence) and T7PS (5′-TTAATACGACTCACTATAGG-3′; plus-strand sequence). The two fragments were mixed and used as template for a second PCR with 283 MS and T7PS as the outside oligonucleotides. The resulting fragment was cut with restriction enzymes Bpu1102 and PmlI and ligated into plasmid GG PV1(M), previously cut with the same restriction enzymes.

In GA sPV1(M) cDNA, the EcoRI-AgeI fragment of sPV1(M) was replaced by the respective EcoRI-AgeI fragment of GA PV1(M) to introduce the G-to-A reversion at position 103.

In vitro transcription, transfection, and virus isolation. All plasmids were linearized with EcoRI. RNAs were synthesized with phage T7 RNA polymerase, and the RNA transcripts were transfected into HeLa R19 cell monolayers by the DEAE-dextran method, as described previously (57). Upon exhibiting complete cytopathic effect, cell monolayers were subjected to three cycles of freezing and thawing in culture medium. The viruses were plaque purified, and the titer was determined by a standard plaque assay (41). HeLa cells were infected with plaque-purified virus at a multiplicity of infection (MOI) of 10 PFU/cell. The supernatants were titrated and used as virus stocks.

RNA extraction, RT-PCR, and DNA sequencing. Genomic sequences were derived from total RNA of poliovirus-infected HeLa cells. HeLa cells were either infected with virus stocks or virus populations recovered from the spinal cord of poliovirus-infected *CD155* tg mice (see below). RNA extracted from infected HeLa cells using TRIzol solution (Invitrogen) served as template for reverse transcription-PCR (RT-PCR). In this manner, poliovirus-specific amplicons were designed to cover the entire poliovirus genome. The RT-PCRs were performed using the Titan One-Tube RT-PCR system following the manufacturer's instructions (Roche Mannheim), and the PCR amplicons were purified with the QIAquick gel extraction kit (QIAGEN). The full-length genome sequence of the purified PCR products was determined with oligonucleotide primers in cycle sequencing (ABI Prism BigDye terminator cycle sequencing ready reaction kit; Applied Biosystems) in an automated sequencer (model 310; Applied Biosystems).

Neurovirulence assays in mice. Groups of four to six *CD155* tg mice (equal numbers of males and females) were inoculated with a given amount of virus ranging from 10^2 to 10^8 PFU (30 μl/mouse) intracerebrally for the different poliovirus strains studied here. Mice were examined daily for 21 days postinoculation for paralysis and/or death. The virus titer that induced paralysis or death in 50% of the mice (PLD_{50}) was calculated by the method of Reed and Muench (44). Homogenized spinal cord specimens were prepared from paralyzed mice for each virus tested, and the isolated viruses were amplified in HeLa cells. Viral isolates were purified by plaque assay in monolayer cultures of HeLa cells, and virus stocks were prepared as described above. These virus stocks were used for sequencing reactions. All procedures involving experimental mice were conducted according to protocols approved by the institutional committees on animal welfare.

One-step growth curves at 37°C and 39.5°C. One-step growth curves in HeLa cells and SK-N-MC neuroblastoma cells at 37°C and 39.5°C were carried out as follows. Cell monolayers in 35-mm plastic culture dishes were washed with Dulbecco's minimal essential medium (DMEM) and inoculated at an MOI of 10 with the virus to be tested. After the dishes were rocked for 30 min at room temperature, the cells were thoroughly washed to remove unbound virus and placed at 37°C or 39.5°C. At 0, 2, 4, 6, 8, 12, and 24 h postinfection, the dishes were subjected to three consecutive freeze-thaw cycles, and the viral titers of the supernatants were determined by plaque assay, as described before (41).

Preparation of HeLa and SK-N-MC cell extracts. HeLa S10 cell extracts were prepared as previously described (8, 32) except for the following modifications: (i) packed cells from 2 liters of HeLa S10 were resuspended in 1 volume (relative to packed cell volume) of hypotonic buffer, and (ii) the final extracts were not dialyzed. SK-N-MC extracts were prepared as described for HeLa S10 cell-free extract except for the following modification: 20 15-cm-diameter plates of SK-N-MC grown to confluence were used to obtain 2 ml of extract. The cells were detached by brief washing with trypsin-EDTA and further incubation with a fresh portion of trypsin-EDTA at 37°C for 3 min. Trypsinization was stopped by adding 10 ml 10% fetal bovine serum in DMEM. Cell aggregates were disrupted by pipetting, and the cell suspension was transferred to a centrifuge tube containing cold 10% fetal bovine serum in DMEM. The cells were collected by centrifugation, washed three times with phosphate-buffered saline, and processed for the preparation of the extract, as described for HeLa cells. The cell viability of SK-N-MC cells after trypsinization was shown to be greater than 90% by trypan blue exclusion test.

In vitro translation of viral mRNAs. Plasmid DNAs were linearized with EcoRI and transcribed with phage T7 RNA polymerase (57). The RNAs were purified by phenol-chloroform extraction and ethanol precipitation. The purified RNAs were translated in either HeLa or SK-N-MC cell extracts in the presence of Tran^{35}S-label (ICN Biochemicals). The reaction mixtures were incubated at 34°C for 15 h (32). Samples of the translation reaction mixtures were analyzed on sodium dodecyl sulfate-polyacrylamide gels with 12.5% acrylamide. The gels were dried and subjected to autoradiography. The data were analyzed with the program Image J (National Institutes of Health [NIH]). The translation efficiency of each mutant RNA in HeLa or SK-N-MC cell extracts was expressed as a percentage of VP3 protein observed relative to wt PV RNA transcript in each cell extract.

RESULTS

We have followed two strategies to identify the mutation(s) responsible for the attenuation phenotype of sPV1(M). One was an exchange of genomic segments of the viral strains sPV1(M) and PV1(M) with subsequent analyses of neurovirulence. The other was to rescue virus from the spinal cord of sPV1(M)-infected *CD155* tg mice that expressed pathology. We reasoned that virus strains isolated from diseased animals may have reverted to a neurovirulent phenotype, thereby revealing the locus of attenuation.

In any case, the cDNAs of parental viruses or of genetically engineered derivatives were transcribed with T7 RNA polymerase, and the isolated RNAs were transfected into HeLa cell cultures. After one passage, the progeny viruses were sequenced in toto to ascertain the genotypes of the isolates. Analysis of the sequence of sPV1(M) RNA showed, as predicted, the presence of the 27 nucleotide substitutions that we had engineered into this genome to distinguish it from the sequence of PV1(M) (7).

Exchange of genome segments between sPV1(M) and PV1(M). In our initial experiments to determine the location of the attenuating mutations in the genome of sPV1(M), we exchanged the 5′-terminal 3,836-nucleotide-long segment between this strain and the highly neurovirulent PV1(M) (see Materials and Methods). Passage of these viral variants, termed sPV1(M)-PV1(M) and PV1(M)-sPV1(M), in HeLa cells showed genotype stability. Their neurovirulent phenotype was analyzed by intracerebral inoculations of *CD155* tg mice. When three mice were inoculated with either 10^6 or 10^3 PFU of PV1(M)-sPV1(M), respectively, all six animals succumbed. In contrast, the inoculation of mice with 10^6 and 10^3 PFU of sPV1(M)-PV1(M) resulted in death of one out of three animals and zero out of three animals, respectively. These results indicate that the mutations engineered in the 5′-half of PV1(M) contributed significantly to the attenuation phenotype of sPV1(M).

TABLE 1. Neuropathogenicity of sPV1(M), PV1(M), and their mutant and revertant viruses in CD155 tg mice

Virus	Nucleotides at positions 102 and 103	PLD_{50} (log_{10} PFU)[a]
sPV1(M)	GG	5.8
GA sPV1(M)	GA	2.6
UA sPV1(M)	UA	2.0
GG PV1(M)	GG	5.9
GA PV1(M)	GA	2.0
PV1(M)	UA	1.9

[a] PLD_{50} is defined as the amount of virus that caused paralysis or death in 50% of the inoculated mice.

Isolation of rescued viruses from sPV1(M)-infected *CD155* tg mice. The data obtained so far indicated that the locus of the attenuation phenotype of sPV1(M) maps to the 5′-half of the sPV1(M) genome. The identity of the attenuating mutation was then revealed by sequencing virus isolates that had been rescued from the spinal cord of those *CD155* tg mice infected with sPV1(M) that showed symptoms of neurological disease (see Materials and Methods). Full genomic sequencing of virus variants recovered from the spinal cord of mice infected with sPV1(M) demonstrated a single reversion: the transition of the G residue at nt 103 to an A residue. This reversion was observed in five out of the five plaque-purified viruses isolated from diseased mice originally inoculated with poliovirus carrying GG nucleotides at the 102/103 locus.

Neurovirulence of revertant viruses in *CD155* tg mice. To identify the contribution of the mutations at the 102/103 locus to attenuation, we tested wt, mutant, and revertant viruses for their neuropathogenic phenotypes by intracerebral inoculation of *CD155* tg mice. For this purpose, we constructed several viral variants with mutations at the 102/103 locus: sPV1(M) variants with the partially reverted sequence (GA) or the wt sequence, referred to as GA sPV1(M) and UA sPV1(M), respectively, and derivatives of PV1(M), referred to as GG PV1(M) and GA PV1(M), respectively. These variants showed stable genotypes when passaged in HeLa cells.

Analysis of neurovirulence tests in *CD155* tg mice revealed that the PLD_{50} values of the two viruses containing the $G_{102}G_{103}$ mutations, sPV1(M) and GG wt PV1(M), were ~4 log_{10} higher than those of UA sPV1(M) and wt PV1(M), two genotypes with a wt UA dinucleotide at 102/103 (Table 1).

We then determined the PLD_{50} values of the GA sPV1(M) and GA PV1(M) variants. They were found to be $>10^3$-fold lower than those of sPV1(M) and GG PV1(M), respectively (Table 1). This observation indicates that the reversion of G to A at position 103 alone is capable of dramatically increasing the neurovirulence of the revertant viruses. Since the revertant viruses showed PLD_{50} values which were similar, albeit not identical, to those of the viruses carrying UA at 102/103 (Table 1), we conclude that G at position 103 is the main contributor to the attenuated phenotype of sPV1(M) and GG PV1(M).

Polioviruses carrying $G_{102}G_{103}$ exhibit a ts phenotype in human neuroblastoma cells. To determine the growth phenotypes of sPV1(M), GG PV1(M), and UA sPV1(M) and to compare these with those of PV1(M), one-step growth curve experiments were carried out with these viruses at 37°C and 39.5°C in HeLa cells and in SK-N-MC, a human cell line of neuronal origin (5). Analysis of the growth curves showed that all poliovirus variants replicated well in HeLa cells at the two temperatures, regardless of the sequence at the 102/103 locus, e.g., GG PV1(M) and sPV1(M), and also UA sPV1(M) (Fig. 2A and B). Indeed, the variants replicated with nearly identical kinetics as wt PV1(M).

We then determined the growth properties of these viruses in SK-N-MC cells. At 37°C, the parental and mutant viruses reached the highest titer approximately 24 h postinfection, a considerable delay in comparison to replication in HeLa cells (highest viral titers are generally between 6 and 12 h postinfection) (compare Fig. 2A with 3A). Thus, under the conditions of the experiments, the neuronal cells did not provide maximal conditions for poliovirus production.

Although the one-step growth curves indicated that all poliovirus variants tested replicated in SK-N-MC cells at 37°C, the maximum titers of variants carrying GG at the 102/103 locus, i.e., sPV1(M) and GG PV1(M), were approximately 1 log_{10} unit lower than those of UA sPV1(M) and PV1(M) (Fig. 3A). Remarkably, at 39.5°C the viral variants sPV1(M) and GG PV1(M) hardly replicated at all in neuroblastoma cells (Fig. 3B). Polioviruses with a UA base pair at locus 102/103, on

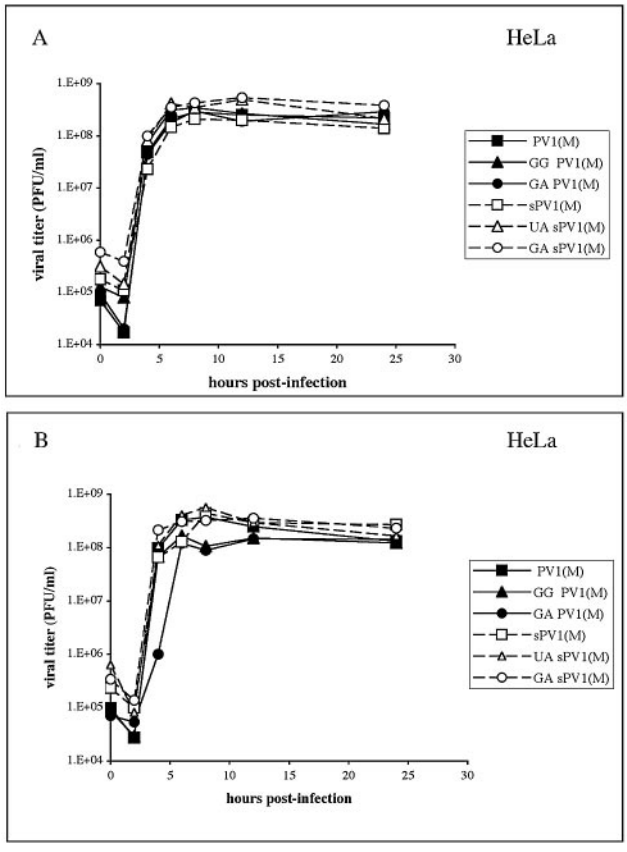

FIG. 2. One-step growth curve analysis of poliovirus strains in HeLa cells. Cells were infected at an MOI of 10 and incubated at 37°C (A) or 39.5°C (B). The virus titer was determined by plaque assay on monolayers of HeLa cells, as described in Materials and Methods. Each point represents the mean of virus titers from three different experiments.

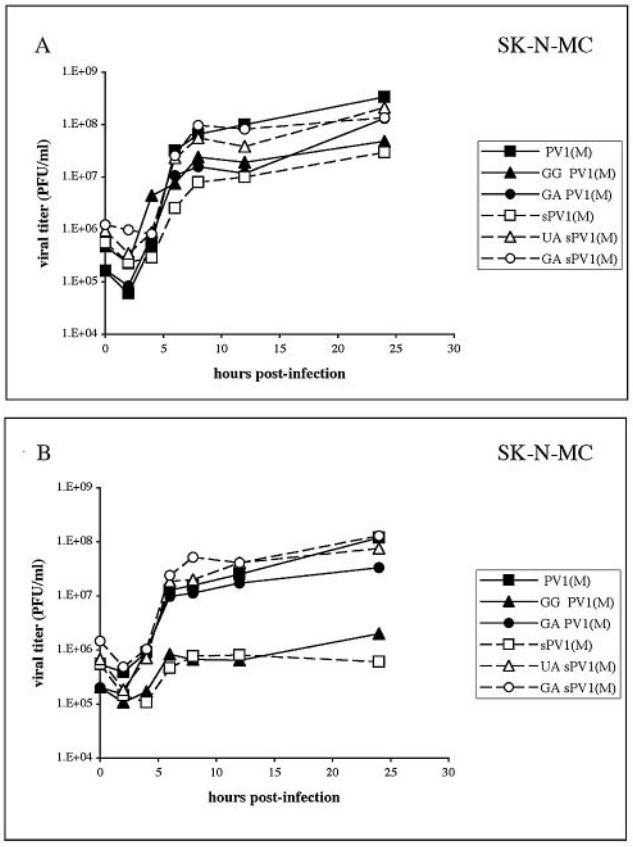

FIG. 3. One-step growth curve analysis of poliovirus strains in SK-N-MC cells. Cells were infected at an MOI of 10 and incubated at 37°C (A) or 39.5°C (B). The virus titer was determined by plaque assay on monolayers of HeLa cells, as described in Materials and Methods. Each point represents the mean of virus titers in three different experiments.

the other hand, retained efficient growth in this cell line at 39.5°C (Fig. 3B). Altogether, these data provide strong evidence that mutations at the 102/103 locus in the 5′NTR of poliovirus lead to a ts growth phenotype in human cells of neuronal origin.

The G-to-A reversion at position 103 suppresses the ts phenotype of sPV1(M) and GG PV1(M) in SK-N-MC cells. We have previously observed that virus isolated from the spinal cord of paralyzed mice infected with sPV1(M) harbored only one nucleotide change with respect to the parental virus, e.g., a reversion of G to A at 103 (see above). This identical and unique change was also detected in virus isolated from the spinal cord of paralyzed mice inoculated with GG PV1(M). To characterize the growth phenotype conferred by this reversion at position 103, the growth kinetics of GA sPV1(M) and GA PV1(M) were determined. Plaque-purified isolates of either variant were assayed in HeLa and SK-N-MC cells at 37°C and 39.5°C. As shown in Fig. 2A and B, both variants grew well in HeLa cells at the two temperatures tested.

GA sPV1(M) and GA PV1(M) also replicated efficiently in SK-N-MC cells at 37°C, as evidenced by one-step growth experiments (Fig. 3A). At this temperature, the final yield of the revertant viruses approached that of PV1(M) and UA sPV1(M), two viruses with a wt UA dinucleotide pair at the 102/103 locus (Fig. 3A). Remarkably, GA sPV1(M) and GA PV(M) also replicated well in SK-N-MC at 39.5°C, displaying growth phenotypes similar to that of PV1(M) and UA sPV1(M) (Fig. 3B). These results suggest that the reversion of G to wt A at position 103 was sufficient to overcome the ts phenotype of poliovirus mutants with a GG pair at the 102/103 locus. Interestingly, the loss of the ts phenotype in SK-N-MC cells covaried with the loss of neurovirulence in *CD155* tg mice.

Nucleotide sequence alignment of the spacer region between the cloverleaf and the IRES of polioviruses. Nucleotides 102 and 103 are localized in a relatively unstructured spacer region of approximately 35 nt that connects the end of the cloverleaf and the beginning of the IRES (Fig. 1). Nucleotide sequence alignment analysis showed that this region has many conserved nucleotides among poliovirus serotypes, including an A at position 103 (Fig. 4). The presence of a high degree of nucleotide conservation in this segment of the poliovirus genome suggests a function for this region. Moreover, the AACUUAGA octanucleotide is highly conserved among the majority of the C-cluster coxsackie A viruses, which are closely related to poliovirus (Fig. 4).

In vitro translations of viral mRNAs in HeLa and SK-N-MC cell extracts. To determine whether the reduced growth phenotypes of $G_{102}G_{103}$ viruses in neuronal cells may be related to a defect in translation, we have begun to test the translational efficiencies of wt and mutant viral RNAs in HeLa and SK-N-MC cell extracts. Generally, the translation of each RNA tested appeared to be more efficient in HeLa than in SK-N-MC cell extracts (Fig. 5). This difference is apparent even with PV1(M) RNA (Fig. 5, compare lanes 5 and 6), the wt poliovirus RNA previously shown to initiate a complete translation/replication/encapsidation cycle in HeLa cell extracts (32). Extremely poor translation in SK-N-MC extracts, in comparison to HeLa cell extracts, was observed with all viral RNAs carrying GG at locus 102/103 (compare lanes 1 and 2 and lanes 7 and 8). In SK-N-MC cells, the efficiency was reduced to 20% and 36% for GG PV1(M) and sPV1(M), respectively, compared to translation of RNAs carrying the UA sequence at 102/103 (Fig. 5, compare lane 1 with lane 5 and lane 7 with 9). Indeed, recovery was even achieved with the variants of PV1(M) and sPV1(M) RNAs in which only G_{103} had been changed to the wt A residue (compare lane 1 with 3 and lane 7 with 11, respectively). Overall, our findings indicate that the differences in translation efficiencies of RNAs observed in the cell extracts correlated with differences in growth phenotypes of the viruses in HeLa and SK-N-MC cells. Remarkably, the G-to-A reversion at position 103, which correlated with the suppression of the ts phenotype in SK-N-MC cells and restoration of the wt neurovirulence in *CD155* tg mice of poliovirus mutants with a GG pair at the 102/103, significantly increased the translation efficiency of the poliovirus RNAs in neuronal cell extracts.

DISCUSSION

The 5′NTR of poliovirus has a modular organization in which the cloverleaf and the IRES regulate primarily RNA replication and viral protein synthesis, respectively (1, 16, 58). Nucleotide changes in these RNA structures can have a pro-

Serotype	8 9	1 1 0 0 2 3	1 2 3	GenBank accession no. (Reference)
sPV1(M)	UACUCCCUUCC C	GGGACUU AGACGCACA	AAA C C AA	(7)
PV1(M)	UACUCCCUUCC C	GUAACUU AGACGCACA	AAA C C AA	V01149 (24, 43)
PV1(S)	---------- -	------- ---------	--- - - --	AY184219 (46)
PV1-F1	---------- -	-C----- -------U-	---A- - --	AJ132960 (4)
PV1-F2	---------- -	-A----- -------UG	--- - -C--	AJ132961 (4)
PV2(La)	-------U--- -CG	-U----- ---A----A	-UGU- - --	M12197 (27)
PV2(S)	-------C--- -	-C----- ---A----G	--- - - --	AY184220 (47)
PV2-F1	-------C--- -	-C----- ---A----G	--- - - --	AY278549 (26)
PV2-F2	-------C--- -	-C----- ---A----G	--- - - --	AY278550 (26)
PV3(Le)	--------C-- -C	-C----- ---A---U-	C--UU - --	K01392 (52)
PV3(S)	--------C-- -C	-C----- ---A---U-	C--UU - --	AY184221 (48)
PV3-F1	---------- -C	------- ---A-U-U-	C--G- - --	X04468 (17)
CAV1	--UC----C-- -AA	-------U---A---AU	UC- - A --	AF499635 (6)
CAV11	--------C-- -C	------- ---A---AUC	--- U - --	AF499636 (6)
CAV13	--UC------- -CC	-C----- ---A-UUAU	--- - - --	AF499637 (6)
CAV15	--------C-- -CCC	------- ---A-U---	--- -U- --	AF499638 (6)
CAV17	---------- -CC	------- ---A---AUC	--- - A --	AF499639 (6)
CAV18	C---------- -C	------- -------AU	--- - - --	AF499640 (6)
CAV19	C---------- -UAC	-C-----U---A-UUU-	-C- U A --	AF499641 (6)
CAV20	--------C--U -	------- ---A-----	--- - - --	AF499642 (6)
CAV21	-- --------- -CC	-------U---A--UU-	UC- A	--	AF546702 (6)
CAV22	--UC----C-- -UGA	-------U---A---AU	UC- A A -G	AF499643 (6)
CAV24	A-------C-- -C	---G--- ---A-----	--C A A --	D090457 (53)

FIG. 4. Nucleotide sequence alignment of the region between the cloverleaf and the IRES of polioviruses and human C-cluster coxsackie A viruses. Dashes represent nucleotides conserved in comparison to the PV1(M) sequence. Spaces denote nucleotides missing in PV1(M) but that are otherwise present in other polioviruses or members of the human C-cluster coxsackie A viruses. An octanucleotide that is highly conserved among the polioviruses and coxsackieviruses has been underlined in the PV1(M) sequence. Nucleotides at position 102 and 103 are shown in bold. M, Mahoney; S, Sabin; La, Lansing; Le, Leon; F1 and F2, field isolates 1 and 2.

found effect on the replication phenotype and/or pathogenic properties of polioviruses (13, 58). The work described here shows that mutations in the nucleotide sequence which separates the cloverleaf from the IRES also affect the biological properties of the virus variant. Indeed, we report that this spacer region carries an important functional element that so far had escaped detection.

The novel finding is based on phenotypic analyses of a synthetic poliovirus [sPV1(M)] whose genome harbors 27 nucleotide substitutions compared to the genome of PV1(M) (7). Two phenotypes of sPV1(M) revealed the importance of the spacer region between the cloverleaf and the IRES element. The first was the highly attenuated phenotype of sPV1(M) in *CD155* tg mice, and the second was the ts phenotype of sPV1(M) replication in human neuronal cells (SK-N-MC cells).

Genetic analyses described here have allowed us to unambiguously conclude that of the 27 nucleotide substitutions engineered into sPV1(M), the GG mutations at locus 102/103 are solely responsible for the attenuation phenotype and temperature sensitivity of sPV1(M) in neuroblastoma cells. First, the exchange of GG to wt UA at the 102/103 positions in an sPV1(M) background suppressed the ts phenotype in SK-N-MC cells and restored the wt neurovirulence in *CD155* tg mice. Second, the exchange of wt UA to GG at the 102/103 locus in a PV1(M) background conferred to the mutant a ts phenotype in the neuronal cell line and a highly attenuated phenotype for neurovirulence in *CD155* tg mice.

The search for revertants in paralyzed *CD155* tg mice has further narrowed the genetic locus of *ts* and attenuation. Remarkably, a G-to-A reversion at position 103 was the only nucleotide change observed in the genome of viruses recovered from the spinal cords of paralyzed mice inoculated with sPV1(M) or with GG PV1(M). This finding indicates that motor neurons of *CD155* tg mice exerted a selective pressure on two polioviruses carrying GG at locus 102/103 to revert the G residue to an A residue, and only to this A residue, at position 103. Furthermore, revertant viruses [GA sPV1(M) and GA PV1(M)] had acquired the neurovirulent and growth phenotype of PV1(M). These data strongly suggest that the $G_{103}A$ direct back reversion was necessary and sufficient to restore the neurovirulence typical of PV1(M) and to suppress the ts phenotype in neuronal cells conferred by the $G_{102}G_{103}$ mutations (Fig. 2B and 3B). Collectively, our data show that the ts phenotype in SK-N-MC cells correlates with an attenuation phenotype of poliovirus in *CD155* transgenic mice. Fittingly, PV1(RIPO), a chimeric virus in which the cognate IRES was exchanged to that of human rhinovirus 2, is not only highly

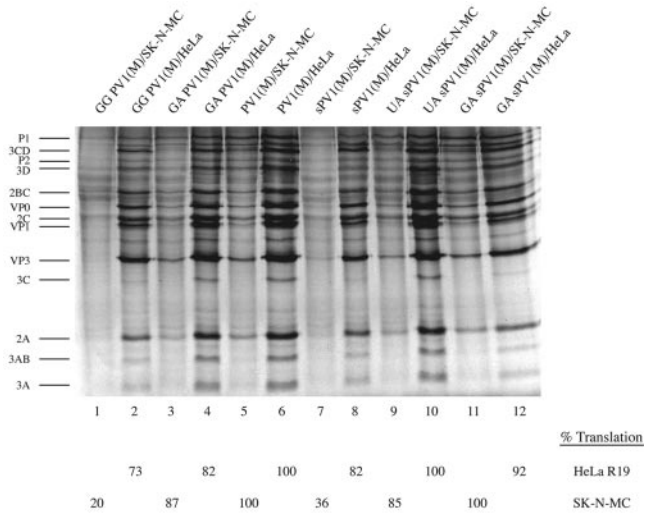

FIG. 5. Products of in vitro translation and proteolytic processing of poliovirus RNAs in HeLa and SK-N-MC cell extracts. Transcript RNAs derived from PV1(M), sPV1(M), and their derivatives were translated and analyzed in HeLa or SK-N-MC cell extracts as indicated (see Materials and Methods). Differences in translation efficiencies among mutant RNAs in HeLa or SK-N-MC cell extracts were revealed by the percentage of VP3 protein generated by translation in each cell extract relative to that obtained for PV1(M) (100%). Bands correspond to segments of the poliovirus polyprotein following proteolytic processing. VPO, 2BC, 3AB, and $3CD^{pro}$ are precursor polypeptides.

attenuated in *CD155* tg mice (11, 12) but is also highly ts in SK-N-MC cells (S. Mueller, N. Jahan, R. Welker, H. Toyoda, J. Cello, and E. Wimmer, unpublished data). These observations support a previous suggestion that neuroblastoma cells may serve as a tissue culture model for studying poliovirus neurovirulence (2, 28), although caution should be exercised not to generalize this association. On the other hand, it is important to note that the exchange of the IRES in PV1 (RIPO) is done by modifying conserved nucleotides localized in the region between the cloverleaf and the IRES of poliovirus. In view of the findings described here, we are presently examining the contribution of these modifications to the attenuated phenotype of PV1(RIPO).

An alignment of the spacer region between the cloverleaf and the IRES for many of the known polioviruses indicates variable as well as highly conserved regions (Fig. 4). With respect to the 102/103 locus, A_{103} is completely conserved and so are seven other bases downstream of nt 103 (A_{103}ACUUA GA_{110}). However, mutations of bases other than G_{103}, which could serve as second site suppressors, have not been observed, a result in support of the importance of the 103 locus. Sequence analyses of the genomes of vaccine-derived viruses and field poliovirus isolates showed that base substitutions are frequent at position 102 while the A residue at position 103 is invariable (4, 42). These findings indicate that the conservation of an A residue at position 103 in the 5′NTR is critical for efficient replication of polioviruses.

Among the enteroviruses, the C-cluster coxsackie A viruses are most closely akin to poliovirus (18, 34, 35). Their genomic sequences have been recently determined (6; P. Jiang, H. Shimizu, E. Rieder, and E. Wimmer, unpublished data). Interestingly, among the majority of the C-cluster coxsackie A viruses, the AACUUAGA octanucleotide is also conserved. However, this region harbors many base changes in other enterovirus genomes. Nevertheless, an alignment of all known enterovirus sequences indicates complete conservation of an A residue corresponding to poliovirus A_{103} (36). Whether changes of this A residue in the genome of other enteroviruses will yield phenotypes such as host cell-dependent temperature sensitivity is currently under investigation.

What is the molecular basis for the attenuation and ts phenotypes of the sPV1(M) and GG PV1(M) viruses, which harbor $G_{102}G_{103}$? We do not yet have an explanation, but the inefficiency by which the GG-variant RNAs are translated in cell extracts of SK-N-MC cells suggests that the mutation at the 103 locus downregulates protein synthesis in cells of neuronal origin. This effect is host cell specific, since genomic RNAs of the different virus derivatives, regardless of the genotype of their spacer region, translate well in HeLa extracts, albeit not with the same efficiency as wt PV1(M) (Fig. 5). Further work to substantiate the effect of the 102/103 mutations on translation is in progress.

Nomoto and colleagues have introduced mutations into domain II of the poliovirus IRES, resulting in growth and neurovirulence phenotypes (19, 20, 49, 50). These phenotypes could be suppressed by two concurrent second-site mutations, one at different sites in domain II and the other always at nt 107 in the spacer region. Interestingly, the nt 107 suppressor mutation maps to the highly conserved octanucleotide described in Fig. 4. In contrast to these studies, the single mutation at the nt 103 locus, described here, was sufficient to change the growth and neurovirulence phenotypes of PV, and second-site suppressor mutations have not been observed.

Mutations in a different part of the poliovirus IRES exert also phenotypes that covary with host range, translation, and pathogenesis. For example, it has been shown that a single attenuating mutation in domain V of the IRES elements of the Sabin PV vaccine strains correlates with reduced translational efficiencies and restricted growth in neuronal cells but not in HeLa cells (2, 28, 54, 55). In a different study, a host-range cell-dependent phenotype has been observed with PV1(M) in which domain V of the IRES was mutated by linker insertion and reversion (15). Specifically, some genetic variants in domain V were restricted in growth in neuroblastoma cells while growing normally in HeLa cells (15). It has been speculated that neuronal cells may be lacking, or contain a suboptimal supply of, a host factor necessary for translation of the mutated viral RNA. This factor may be in ample supply in HeLa cells. Experimental evidence supporting this hypothesis has been recently published (14).

Mutations in domain V of the poliovirus IRES map some 377 nt downstream of the spacer region analyzed here (Fig. 1), and their effects may not be related to each other. Long distance interactions between these regions, however, cannot be ruled out.

The large effect of the single nucleotide exchange, $A_{103}G$, on translation in vitro, replication in neuronal cells at elevated temperatures, and virulence in *CD155* tg mice is astounding, as these phenotypes are likely to relate to the same single base locus. Does the A_{103} residue in the spacer interact directly or indirectly (bridged by proteins) with elements of the desig-

nated IRES? One possibility is that the mutations alter the interaction of this region with a translation factor. Alternatively, the mutation at position 102/103 may influence the stability of neighboring IRES structures, resulting in an inefficient interaction of cell type-specific factors and the IRES. If so, the spacer may be a functional element of the IRES that has been ignored simply because of the assays used in studying mutations in this region of the viral genome. Indeed, the use of non-neuronal-based assays for characterization of phenotypic properties of mutated poliovirus strains might have precluded in the past the identification of viral determinants that might profoundly affect the phenotype of poliovirus (38, 56). Finally, since the nucleotides 102 and 103 are localized near the cloverleaf, the possibility cannot be excluded that a mutation at this locus might also modulate cloverleaf activity. Mutations in the cloverleaf have been shown to influence not only genome replication but also viral protein synthesis (51). The mutations studied here might also affect not only the viral translation but also viral RNA replication.

In summary, our results show that the mutation of a conserved nucleotide localized in the region between the cloverleaf and the IRES in the 5′NTR strongly influences the biological properties of poliovirus. Hence, it will be interesting to determine the contribution of other conserved nucleotides in this region to poliovirus pathogenesis.

ACKNOWLEDGMENTS

We thank Steffen Mueller for illuminating discussions and Alex Kenigsberg and Edison Mejia for expert technical assistance.

This work was supported by NIH grants AI15122 and A132100. N. DeJesus is supported by NIH Training grant 5T32CA09176-27 as well as a Medical Scientist Training grant.

REFERENCES

1. **Agol, V. I.** 2002. Picornavirus genome: an overview, p. 127–148. *In* B. L. Semler and E. Wimmer (ed.), Molecular biology of picornaviruses. ASM Press, Washington, D.C.
2. **Agol, V. I., S. G. Drozdov, T. A. Ivannikova, M. S. Kolesnikova, M. B. Korolev, and E. A. Tolskaya.** 1989. Restricted growth of attenuated poliovirus strains in cultured cells of a human neuroblastoma. J. Virol. **63:**4034–4038.
3. **Andino, R., G. E. Rieckhof, and D. Baltimore.** 1990. A functional ribonucleoprotein complex forms around the 5′ end of poliovirus RNA. Cell **63:**369–380.
4. **Bellmunt, A., G. May, R. Zell, P. Pring-Akerblom, W. Verhagen, and A. Heim.** 1999. Evolution of poliovirus type I during 5.5 years of prolonged enteral replication in an immunodeficient patient. Virology **265:**178–184.
5. **Biedler, J. L., L. Helson, and B. A. Spengler.** 1973. Morphology and growth, tumorigenicity, and cytogenetics of human neuroblastoma cells in continuous culture. Cancer Res. **33:**2643–2652.
6. **Brown, B., M. S. Oberste, K. Maher, and M. A. Pallansch.** 2003. Complete genomic sequencing shows that polioviruses and members of human enterovirus species C are closely related in the noncapsid coding region. J. Virol. **77:**8973–8984.
7. **Cello, J., A. V. Paul, and E. Wimmer.** 2002. Chemical synthesis of poliovirus cDNA: generation of infectious virus in the absence of natural template. Science **297:**1016–1018.
8. **Cuconati, A., A. Molla, and E. Wimmer.** 1998. Brefeldin A inhibits cell-free, de novo synthesis of poliovirus. J. Virol. **72:**6456–6464.
9. **Dorner, A. J., L. F. Dorner, G. R. Larsen, E. Wimmer, and C. W. Anderson.** 1982. Identification of the initiation site of poliovirus polyprotein synthesis. J. Virol. **42:**1017–1028.
10. **Flanegan, J., R. Pettersson, V. Ambros, M. Hewlett, and D. Baltimore.** 1977. Covalent linkage of a protein to a defined nucleotide sequence at the 5′-terminus of virion and replicative intermediate RNAs of poliovirus. Proc. Natl. Acad. Sci. USA **74:**961–965.
11. **Gromeier, M., L. Alexander, and E. Wimmer.** 1996. Internal ribosomal entry site substitution eliminates neurovirulence in intergeneric poliovirus recombinants. Proc. Natl. Acad. Sci. USA **93:**2370–2375.
12. **Gromeier, M., B. Bossert, M. Arita, A. Nomoto, and E. Wimmer.** 1999. Dual stem loops within the poliovirus internal ribosomal entry site control neurovirulence. J. Virol. **73:**958–964.
13. **Gromeier, M., and A. Nomoto.** 2002. Determinants of poliovirus pathogenesis, p. 367–379. *In* B. L. Selmer and E. Wimmer (ed.), Molecular biology of picornaviruses. ASM Press, Washington, D.C.
14. **Guest, S., E. Pilipenko, K. Sharma, K. Chumakov, and R. P. Roos.** 2004. Molecular mechanisms of attenuation of the Sabin strain of poliovirus type 3. J. Virol. **78:**11097–11107.
15. **Haller, A. A., S. R. Stewart, and B. L. Semler.** 1996. Attenuation stem-loop lesions in the 5′ noncoding region of poliovirus RNA: neuronal cell-specific translation defects. J. Virol. **70:**1467–1474.
16. **Hellen, C. U. T., and E. Wimmer** 1995. Enterovirus genetics, p. 25–72. *In* H. A. Rotbart (ed.), Human enterovirus infections. ASM Press, Washington, D.C.
17. **Hughes, P. J., D. M. Evans, P. D. Minor, G. C. Schild, J. W. Almond, and G. Stanway.** 1986. The nucleotide sequence of a type 3 poliovirus isolated during a recent outbreak of poliomyelitis in Finland. J. Gen. Virol. **67:**2093–2102.
18. **Hyypia, T., T. Hovi, N. Knowles, and G. Stanway.** 1997. Classification of enteroviruses based on molecular and biological properties. J. Gen. Virol. **78:**1–11.
19. **Ishii, T., K. Shiroki, D. H. Hong, T. Aoki, Y. Ohta, S. Abe, S. Hashizume, and A. Nomoto.** 1998. A new internal ribosomal entry site 5′ boundary is required for poliovirus translation initiation in a mouse system. J. Virol. **72:**2398–2405.
20. **Ishii, T., K. Shiroki, A. Iwai, and A. Nomoto.** 1999. Identification of a new element for RNA replication within the internal ribosome entry site of poliovirus RNA. J. Gen. Virol. **80:**917–920.
21. **Iwasaki, A., R. Welker, S. Mueller, M. Linehan, A. Nomoto, and E. Wimmer.** 2002. Immunofluorescence analysis of poliovirus receptor expression in Peyer's patches of humans, primates, and CD155 transgenic mice: implications for poliovirus infection. J. Infect. Dis. **186:**585–592.
22. **Jang, S. K., M. V. Davies, R. J. Kaufman, and E. Wimmer.** 1989. Initiation of protein synthesis by internal entry of ribosomes into the 5′ nontranslated region of encephalomyocarditis virus RNA in vitro. J. Virol. **63:**1651–1660.
23. **Jang, S. K., H.-G. Kräusslich, M. J. H. Nicklin, G. M. Duke, A. C. Palmenberg, and E. Wimmer.** 1988. A segment of the 5′ nontranslated region of encephalomyocarditis virus RNA directs internal entry of ribosomes during in vitro translation. J. Virol. **62:**2636–2643.
24. **Kitamura, N., B. L. Semler, P. G. Rothberg, G. R. Larsen, C. J. Adler, A. J. Dorner, E. A. Emini, R. Hanecak, J. Lee, S. van der Werf, C. W. Anderson, and E. Wimmer.** 1981. Primary structure, gene organization and polypeptide expression of poliovirus RNA. Nature **291:**547–553.
25. **Koike, S., C. Taya, T. Kurata, S. Abe, I. Ise, H. Yonekawa, and A. Nomoto.** 1991. Transgenic mice susceptible to poliovirus. Proc. Natl. Acad. Sci. USA **88:**951–955.
26. **Korotkova, E. A., R. Park, E. A. Cherkasova, G. Y. Lipskaya, K. M. Chumakov, E. V. Feldman, O. M. Kew, and V. I. Agol.** 2003. Retrospective analysis of a local cessation of vaccination against poliomyelitis: a possible scenario for the future. J. Virol. **77:**12460–12465.
27. **La Monica, N., C. Meriam, and V. R. Racaniello.** 1986. Mapping of sequences required for mouse neurovirulence of poliovirus type 2 Lansing. J. Virol. **57:**515–525.
28. **La Monica, N., and V. R. Racaniello.** 1989. Differences in replication of attenuated and neurovirulent poliovirus in human neuroblastoma cell line SH-SY5Y. J. Virol. **63:**2357–2360.
29. **Lee, Y., A. Nomoto, B. Detjen, and E. Wimmer.** 1977. The genome-linked protein of picornaviruses. I. A protein covalently linked to poliovirus genome RNA. Proc. Natl. Acad. Sci. USA **74:**59–63.
30. **Minor, P.** 1997. Poliovirus, p. 555–574. *In* N. Nathanson (ed.), Viral pathogenesis. Lippincott-Raven, Philadelphia, Pa.
31. **Mirzayan, C. M., and E. Wimmer.** 1992. Genetic analysis of an NTP-binding motif in poliovirus polypeptide 2C. Virology **189:**547–555.
32. **Molla, A., A. V. Paul, and E. Wimmer.** 1991. Cell-free, de novo synthesis of poliovirus. Science **254:**1647–1651.
33. **Mueller, S., E. Wimmer, and J. Cello.** 2005. Poliovirus and poliomyelitis: a tale of guts, brains, and an accidental event. Virus Res. **111:**175–193.
34. **Oberste, M. S., K. Maher, D. R. Kilpatrick, and M. A. Pallansch.** 1999. Molecular evolution of the human enteroviruses: correlation of serotype with VP1 sequence and application to picornavirus classification. J. Virol. **73:**1941–1948.
35. **Oberste, M. S., K. Maher, and M. A. Pallansch.** 1998. Molecular phylogeny of all human enterovirus serotypes based on comparison of sequences at the 5′ end of the region encoding VP2. Virus Res. **58:**35–43.
36. **Palmenberg, A., and J. Y. Sgro.** 2002. Alignments and comparative profiles of Picornavirus genera, p. 149–155. *In* B. L. Semler and E. Wimmer (ed.), Molecular biology of picornaviruses. ASM Press, Washington, D.C.
37. **Parsley, T. B., J. S. Towner, L. B. Blyn, E. Ehrenfeld, and B. L. Semler.** 1997. Poly(rC) binding protein 2 forms a ternary complex with the 5′-terminal sequences of poliovirus RNA and the viral 3CD proteinase. RNA **3:**1124–1134.
38. **Pelletier, J., M. E. Flynn, G. Kaplan, V. R. Racaniello, and N. Sonenberg.** 1988. Mutational analysis of upstream AUG codons of poliovirus RNA. J. Virol. **62:**4486–4492.
39. **Pelletier, J., G. Kaplan, V. R. Racaniello, and N. Sonenberg.** 1988. Cap-independent translation of poliovirus mRNA is conferred by sequence elements within the 5′-noncoding region. Mol. Cell. Biol. **8:**1103–1112.

40. **Pelletier, J., and N. Sonenberg.** 1989. Internal binding of eukaryotic ribosomes on poliovirus RNA: translation in Hela cell extracts. J. Virol. **63:** 441–444.
41. **Pincus, S. E., D. C. Diamond, E. A. Emini, and E. Wimmer.** 1986. Guanidine-selected mutants of poliovirus: mapping of point mutations to polypeptide 2C. J. Virol. **57:**638–646.
42. **Pöyry, T., L. Kinnunen, and T. Hovi.** 1992. Genetic variation in vivo and proposed functional domains of the 5′ noncoding region of poliovirus RNA. J. Virol. **66:**5313–5319.
43. **Racaniello, V. R., and D. Baltimore.** 1981. Molecular cloning of poliovirus cDNA and determination of the complete nucleotide sequence of the viral genome. Proc. Natl. Acad. Sci. USA **78:**4887–4891.
44. **Reed, L. J., and M. Muench.** 1938. A simple method for estimating fifty percent endpoints. Am. J. Hyg. **27:**493–497.
45. **Ren, R., F. Costantini, E. J. Gorgacz, J. J. Lee, and V. R. Racaniello.** 1990. Transgenic mice expressing a human poliovirus receptor: a new model for poliomyelitis. Cell **63:**353–362.
46. **Rezapkin, G. V., K. M. Chumakov, Z. Lu, Y. Ran, E. M. Dragunsky, and I. S. Levenbook.** 1994. Microevolution of Sabin 1 strain in vitro and genetic stability of oral poliovirus vaccine. Virology **202:**370–378.
47. **Rezapkin, G. V., L. Fan, D. M. Asher, M. R. Fibi, E. M. Dragunsky, and K. M. Chumakov.** 1999. Mutations in Sabin 2 strain of poliovirus and stability of attenuation phenotype. Virology **258:**152–160.
48. **Rezapkin, G. V., L. P. Norwood, R. E. Taffs, E. M. Dragunsky, I. S. Levenbook, and K. M. Chumakov.** 1995. Microevolution of type 3 Sabin strain of poliovirus in cell cultures and its implications for oral poliovirus vaccine quality control. Virology **211:**377–384.
49. **Shiroki, K., T. Ishii, T. Aoki, M. Kobashi, S. Ohta, and A. Nomoto.** 1995. A new *cis*-acting element for RNA replication within the 5′ noncoding region of poliovirus type 1 RNA. J. Virol. **69:**6825–6832.
50. **Shiroki, K., T. Ishii, T. Aoki, Y. Ota, W. X. Yang, T. Komatsu, Y. Ami, M. Arita, S. Abe, S. Hashizume, and A. Nomoto.** 1997. Host range phenotype induced by mutations in the internal ribosomal entry site of poliovirus RNA. J. Virol. **71:**1–8.
51. **Simoes, E. A. F., and P. Sarnow.** 1991. An RNA hairpin at the extreme 5′ end of the poliovirus RNA genome modulates viral translation in human cells. J. Virol. **65:**913–921.
52. **Stanway, G., P. J. Hughes, R. C. Mountford, P. Reeve, P. D. Minor, G. C. Schild, and J. W. Almond.** 1984. Comparison of the complete nucleotide sequences of the genomes of the neurovirulent poliovirus P3/Leon/37 and its attenuated Sabin vaccine derivative P3/Leon 12a1b Proc. Natl. Acad. Sci. USA **81:**1539–1543.
53. **Supanaranond, K., N. Takeda, and S. Yamazaki.** 1992. The complete nucleotide sequence of a variant of coxsackievirus A24, an agent causing acute hemorrhagic conjunctivitis. Virus Genes **6:**149–158.
54. **Svitkin, Y. V., S. V. Maslova, and V. I. Agol.** 1985. The genomes of attenuated and virulent poliovirus strains differ in their in vitro translation efficiencies. Virology **147:**243–252.
55. **Svitkin, Y. V., T. Pestova, S. V. Maslova, and V. I. Agol.** 1988. Point mutations modify the response of poliovirus RNA to a translation initiation factor: a comparison of neurovirulent and attenuated strains. Virology **166:** 394–404.
56. **Trono, D., R. Andino, and D. Baltimore.** 1988. An RNA sequence of hundreds of nucleotides at the 5′ end of poliovirus RNA is involved in allowing viral protein synthesis. J. Virol. **62:**2291–2299.
57. **van der Werf, S., J. Bradley, E. Wimmer, F. W. Studier, and J. J. Dunn.** 1986. Synthesis of infectious poliovirus RNA by purified T7 RNA polymerase. Proc. Natl. Acad. Sci. USA **78:**2330–2334.
58. **Wimmer, E., C. U. T. Hellen, and X. M. Cao.** 1993. Genetics of poliovirus. Annu. Rev. Genet. **27:**353–436.
59. **Xiang, W., K. S. Harris, L. Alexander, and E. Wimmer.** 1995. Interaction between the 5′-terminal cloverleaf and 3AB/3CD^{pro} of poliovirus is essential for RNA replication. J. Virol. **69:**3658–3667.
60. **Yogo, Y., and E. Wimmer.** 1972. Polyadenylic acid at the 3′-terminus of poliovirus RNA. Proc. Natl. Acad. Sci. USA **69:**1877–1882.
61. **Zhang, S., and V. R. Racaniello.** 1997. Expression of the poliovirus receptor in intestinal epithelial cells is not sufficient to permit poliovirus replication in the mouse gut. J. Virol. **71:**4915–4920.